

Enhanced cell attachment and osteoblastic activity by P-15 peptide-coated matrix in hydrogels

Hieu Nguyen,^a Jing Jing Qian,^b Rajendra S. Bhatnagar,^b and Song Li^{a,*}

^a Department of Bioengineering and The Center for Tissue Engineering, University of California, Berkeley, CA, USA

^b Laboratory of Connective Tissue Biochemistry, University of California, San Francisco, USA

Received 14 September 2003

Abstract

The cells in bone grow on a composite matrix made up of mineral and organic (mainly type-I collagen) components. In this study, anorganic bone mineral (ABM) particles were coated with a cell-binding domain of type-I collagen (P-15 peptide) to mimic the bone matrix components and suspended in injectable hyaluronate (Hy) hydrogels. The ABM/P-15/Hy was compared to ABM/Hy—the same matrix without P-15 peptide. Osteoblast-like HOS cells migrated through the hydrogels around ABM/P-15 or ABM particles; however, more cells adhered to ABM/P-15/Hy particles, and the cells formed better surface coverage and had more stress fibers on ABM/P-15/Hy. HOS cells cultured on ABM/P-15/Hy had increased osteogenic gene expression for alkaline phosphatase and bone morphogenetic proteins, and deposited more mineralized matrix. Studies with two different hydrogels (carboxymethyl-cellulose and sodium alginate) showed similar enhanced cell attachment and mineralization. The studies suggest that the ABM/P-15 in hydrogels can be used as an injectable biomimetic matrix to facilitate bone repair.

© 2003 Elsevier Inc. All rights reserved.

Keywords: Anorganic bone mineral; Collagen; P-15 peptide; Injectable hydrogel; Cell attachment; Osteogenic gene expression; Mineralization; Bone repair

Autograft, allograft (e.g., deep frozen bone and demineralized bone matrix), and biomaterials (e.g., minerals, bioglass, metals, and polymers) have been widely used to repair bone defects [1]. While autologous bone remains the gold standard, its use is limited because of the morbidity arising from additional surgery and the difficulty in obtaining adequate amounts of bone graft matching in size and other characteristics. Allografts of freeze-dried whole bone have the risk of pathogen transfer and immunogenic responses. Although demineralized bone matrix lacks immediate mechanical support, it acts primarily as an osteoconductive bone substitute.

It is desirable to construct biomimetic matrices that mimic the tissue environment in bone and have osteoinductive capability. A bone substitute graft placed in an osseous host site should facilitate cell adhesion, promote osteoblastic differentiation, elicit deposition of matrix

components, and integrate with the surrounding tissue in composition, architecture, and mechanical property. Biomaterials themselves do not have osseointegrative activity due to the lack of bioactive components on the surfaces. An important improvement in biomaterials would be to enhance its ability to interact with cells by the mechanisms that simulate the interaction of cells with their extracellular matrices (ECM) [2–4], e.g., mimicking the role of collagen.

Collagen comprises >90% of the spatially fixed matrix of bone and is a major regulator of cell adhesion [5,6] and osteogenic differentiation [7–11]. Bhatnagar et al. [12,13] have examined the structure of collagen and identified a potent cell-binding domain of human Type-I collagen in the $\alpha 1(I)$ chain sequence (P-15)⁷⁶⁶GTPGPQGIAGQRGVV⁷⁸⁰. P-15 has a conformation characterized by two stretched β -strands flanking a β -bend formed by the central GIAG residues. Previous studies have shown that anorganic bone mineral (ABM, natural hydroxyapatite) particles coated with P-15 peptides can mimic the bone matrix components and

* Corresponding author. Fax: 1-510-231-5631.

E-mail address: songli@socrates.berkeley.edu (S. Li).

facilitate bone regeneration [12–15]. However, the placement of ABM/P-15 particles and the initial containment of the osseous defect site are difficult. A solution is to use hydrogel to facilitate the delivery of ABM/P-15 particles. As hydrogels may impede the migration of cells, it is essential that the hydrogels used in the formulation do not inhibit the performance of the ABM/P-15. In this study, three types of hydrogels were used as carriers of ABM/P-15 particles. Human osteosarcoma cell (HOS), a widely used osteoblast-like cell line for in vitro testing of cell–material interaction and osteoblastic activity [16–19], was used in our experiments. The effect of ABM/P-15 suspended in hydrogels, primarily in sodium hyaluronate (Hy), was evaluated for cell adhesion, osteoblastic gene expression, and mineralization. Studies using the other two hydrogels, carboxymethylcellulose (CMC) and sodium alginate (alginate), supplemented the performance analysis. All of the hydrogels evaluated were inert biocompatible carriers as shown in the previous studies [20–25]. We showed that ABM/P-15 suspended in different hydrogels promoted cell adhesion, enhanced osteoblastic activity, and increased the deposition of mineralized matrix in comparison with ABM in hydrogels, and can be used as injectable biomimetic matrix for bone repair.

Materials and methods

ABM and ABM/P-15 particulate preparation. Totally de-proteinated porous ABM (natural hydroxylapatite) derived from bovine bone in particulate form (250–420 μm) OsteoGraf/N-300 was obtained from Dentsply Friadent CeraMed (Lakewood, CO). The ABM/P-15 matrix is prepared by sorption of synthetic P-15 (GTPGPQGAGQGRGVV) peptide to anorganic bovine-derived mineral (calcium phosphate) matrix. The synthesis and characterization of P-15 peptide and the analysis of ABM/P-15 have been described previously [13,26].

ABM and ABM/P-15 hydrogel preparation. The ABM and ABM/P-15 particulate matrix were suspended in an inert biocompatible hydrogel to facilitate transport and maintain the particles. Each 1 cm^3 of hydrogel/ABM mixture contains 0.51 g ABM or ABM/P-15 particulate. Three hydrogels, described below, were employed in this study. Hy was from Genzyme (Cambridge, MA) and the Hy gel was formulated with 4% Hy (w/w) in water. Hy hydrogel embedded with ABM particles is shown in Fig. 1A as an example. CMC putty carrier was prepared by mixing 15% glycerine (w/w) with 85% water (w/w) and then combining the mixture with 3.25% CMC (w/w). Alginate was from ProNova (Oslo, Sweden) and the putty was formulated with 0.5 g ABM (or ABM/P-15) and 0.17 g alginate in 0.5 ml water.

Cell culture. Cell culture reagents were from Gibco-BRL except otherwise specified. Osteoblast-like HOS cells were from American Type Culture Collection (Manassas, VA). HOS cells were cultured in α -modified Eagle's medium with 10% fetal bovine serum. Cell cultures were maintained in a humidified 95% air–5% CO_2 incubator at 37 $^\circ\text{C}$. The culture medium was changed every 2–3 days. To culture cells on ABM and ABM/P-15 particles inside hydrogels, the surface of the culture wells was coated with poly-hydroxyethyl methacrylate (poly-HEMA) to prevent non-specific cell attachment. The same amount of hydrogel-suspended ABM or ABM/P-15 was used to cover the poly-HEMA coated surface ($\sim 75 \text{ mg}/\text{cm}^2$). The same number of cells was

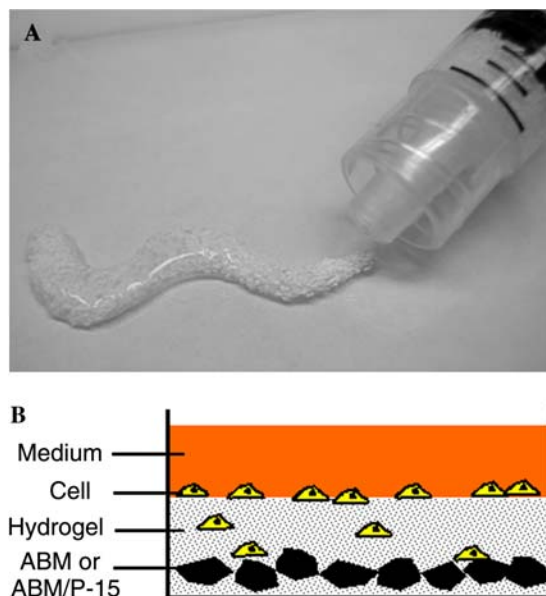


Fig. 1. In vitro experiments using hydrogels. (A) Hy hydrogel embedded with ABM particles. (B) Cell seeding experiments. Hydrogels embedded with ABM particles were spread onto the surface of culture wells. HOS cells were seeded on the hydrogel surface and allowed to migrate into the hydrogel and attach onto the surface of ABM particles.

seeded into each culture well at 60–70% confluence ($\sim 70,000$ cells/ cm^2). This in vitro cell seeding experiment is depicted in Fig. 1B. In this configuration, in order for cells to adhere to the mineral particles, they had to migrate through a layer of hydrogel.

Cell attachment on hydrogel-suspended ABM and ABM/P-15 particles (fluorescence labeling method). To track cells and monitor the cell attachment on hydrogel-suspended ABM and ABM/P-15 particles (non-transparent), HOS cells were labeled with fluorescent dye DiI (Molecular Probes) to allow quantitative measurement of the relative numbers of cells that attached on ABM or ABM/P-15 particles suspended in the hydrogel. DiI is a lipophilic carbocyanine dye (in orange/red color) that stains cell membrane and makes the entire cell visible under fluorescence microscope. DiI has very low cell toxicity. After cell division, DiI retains in cells with decreased amount and intensity. The cells were labeled for 5 min with 10 μM DiI, and seeded into culture wells coated with Hy hydrogel containing ABM or ABM/P-15 (i.e., ABM/Hy or ABM/P-15/Hy). The images of fluorescent cells on the particles were collected at 1, 2, 3, and 4 days by using an upright Zeiss Axioskop 2 fluorescence microscope with an Axiocam camera and an image capture system. The area covered by fluorescent cells in the images was quantified by NIH Image software.

Cell attachment on hydrogel-suspended ABM and ABM/P-15 particles (radioisotope labeling method). An alternative method to label cells was to use [^3H]thymidine. To radiolabel the cells, the HOS cells were cultured in T-75 flasks in MEM containing 10% calf serum. At 50% confluence, the cells were exposed to 0.5 $\mu\text{Ci}/\text{ml}$ [^3H]thymidine (total 20 ml) and the culture was continued for 36 h. The cells were then washed five times with 100 ml phosphate-buffered saline (PBS) containing non-radioactive thymidine (50 $\mu\text{g}/\text{ml}$) (total wash volume 500 ml). The cells were harvested with trypsin and washed two times with PBS-thymidine in the centrifuge and the radioactive content determined in a scintillation counter. The radioactive content of the cells was 6.0×10^7 d.p.m. $^3\text{H}/10^6$ cells.

In order to obtain a quantitative measure of cells migrating to ABM and ABM/P-15 particles embedded in hydrogels (CMC and alginate), 10×10^5 HOS cells biosynthetically radiolabeled with

[^3H]thymidine were placed in the well in a total volume of 1.0 ml of serum-free MEM. The cells were cultured for 24 h. Cells on the ABM substrates were compared with those on the ABM/P-15 substrate. The particles were washed extensively with PBS to remove the hydrogel and non-adherent cells. The particulates with adherent cells were carefully transferred to scintillation counting vials. Radioactivity was determined in a Packard TR-1900 scintillation counter after the cells were solubilized in the counting medium. Multiple counts were recorded and the averaged data for each sample were then subjected to a simple Student's *t* test and plotted as means \pm SE.

MTT (3-(4,5-dimethylthiazolyl-2)-2,5-diphenyltetrazolium bromide) assay. An MTT assay kit (from American Type Culture Collection) was used to measure cell viability and metabolic activity. After certain period of culture, MTT reagent was added to the culture medium for 4 h until purple precipitate was visible. Then detergent reagent was added to the samples and incubated for 2–4 h. The absorbance at 570 nm for each sample was measured by using a Bio-Rad 550 microplate reader.

Actin staining and confocal microscopy. The cells were fixed in 4% paraformaldehyde in PBS for 15 min, followed by permeabilization with 0.5% Triton X-100 in PBS for 10 min. For actin staining, the specimens were stained with FITC-conjugated phalloidin (5 U/ml, Molecular Probes, Eugene, OR) for 1 h. The images of actin structure were collected as Z-series sections with a Leica confocal microscopy system with argon and He/Ne laser sources, a TCL-SL scanner, and a Leica DM IRB microscope. Multiple sections (0.3- μm thick for each section) were projected onto one plane for presentation. FITC was excited at a wavelength of 488 nm and detected within a band between 506 and 538 nm.

Gene expression analysis. Quantitative polymerase chain reaction (qPCR) was used to compare the relative levels of gene expression. The complete gene sequence and cDNA sequence for each gene were downloaded from GenBank. The primers for qPCR were designed by

using Primer Express (Applied Biosystems, Foster, CA). To ensure the PCR specificity, at least one primer for each gene was designed to span a junction of two exons. The primers for glyceraldehyde-3-phosphate-dehydrogenase (GAPDH) were 5'-GAAGGTGAAGGTCGGAGTC-3' (forward) and 5'-GAAGATGGTGATGGGATTTC-3' (reverse). The primers for alkaline phosphatase (ALP) were 5'-TGGAGC TTCAGAAGCTCAACAC-3' (forward) and 5'-TGGAGACACCC ATCCCATCT-3' (reverse). The primers for bone morphogenetic protein 2 (BMP-2) were 5'-CCATGTGGACGCTCTTTCAA-3' (forward) and 5'-GCCACCATGGTCGACCTTTA-3' (reverse). The primers for BMP-7 were 5'-CGTCAACCTCGTGAACATG-3' (forward) and 5'-CAAACCGGAAGTCTCGATGGT-3' (reverse).

To isolate RNA from cultured cells, the cells were lysed in phenol-containing STAT60 lysis buffer (TEL-TEST, Friends Wood, TX). After mixing the lysates with chloroform, RNA was isolated from the aqueous phase by isopropanol precipitation. The contents of RNA were determined by measuring the absorbance at 260 and 280 nm. Equal amounts of total RNA from each sample were reverse-transcribed into cDNAs with ThermoScript (Invitrogen) and mixed with primers, SYBR-green dye, and other components in the SYBR-green kit (Applied Biosystems). Real time qPCR analysis of several genes was performed in parallel in a 96-well format on an ABI 7000 SDS machine. By loading equal amount of total RNA, we showed that GAPDH level did not change significantly in different samples. Therefore, the amount of each gene was normalized with the amount of GAPDH in the same sample.

Alizarin Red staining for mineralization. Positive staining with Alizarin Red is an indicator of mineralization. Culture cells were washed with PBS and fixed in 4% paraformaldehyde for 10 min. The fixed cells were then washed in water and stained with 2% Alizarin Red S in de-ionized distilled water (pH 4.2 by adding ammonium peroxide) for 5 min. The samples were washed to remove excess stain and examined under a stereomicroscope.

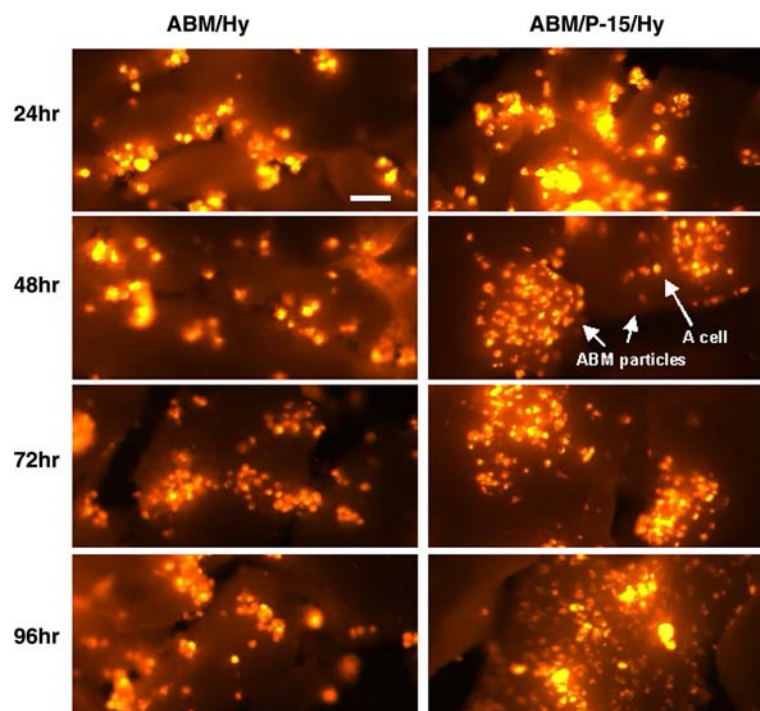


Fig. 2. Effect of P-15 on cell attachment and spreading on the ABM surface in Hy hydrogels. HOS cells were labeled with DiI for 5 min and plated on either ABM/Hy or ABM/P-15/Hy. The images of fluorescent cells on the surface of the particles were collected by fluorescence microscopy at 24, 48, 72, and 96 h. The edge of the ABM particles can be distinguished from the dark background as exemplified in the figure (pointed by arrows). Cells labeled with DiI are shown either as individual spots or as clusters. Bar = 100 μm . Images are representatives of three experiments.

Results

Increased cell attachment on ABM/P-15/Hy

The time course of cell migration through Hy hydrogels and subsequent attachment on ABM particles were determined by labeling HOS cells with DiI fluorescence dye. Fluorescence microscopy was used to monitor the cells at different focus planes. As shown in Fig. 2, cells had reached ABM surface after 24 h and more cell attachment was observed on the ABM/P-15 surface. After 48 h, cell seeded on ABM/Hy showed patches of cell coverage on the ABM surface. On the ABM/P-15 surface in hydrogel, more cell coverage and cell scattering were observed, suggesting that P-15 peptide on ABM surface promotes more cell migration.

Quantification of particle surface area covered by fluorescent cells was determined using NIH Image software to outline the fluorescent cells on particle surface and measure the total area. As shown in Fig. 3A, cell attachment on ABM/P-15 in hydrogel was significantly more ($p < 0.05$) than that on ABM in hydrogel

after 24 h, suggesting that P-15 still enhances cell adhesion on the ABM surface in the presence of Hy hydrogel. This difference was maintained within the time window (4 days) of our experiments (data not shown).

MTT assay was used to compare HOS cell viability on ABM/Hy and ABM/P-15/Hy. As shown in Fig. 3B, after 4-day culture, cell viability was about twofold higher for cells grown on ABM/P-15/Hy, which is consistent with the results on cell attachment (Fig. 3A).

Increased actin filaments and stress fibers with ABM/P-15/Hy

Besides the difference in cell attachment on ABM/Hy and ABM/P-15/Hy, the adhesion quality on the particle surface is also modulated by the presence of P-15. HOS cells were seeded on ABM and ABM/P-15 with or without Hy hydrogel. After 24 h, cells were fixed, stained, and imaged by confocal microscopy (Fig. 4). Cells on ABM surface (with or without hydrogel) had minimal spreading and little stress fibers, suggesting that cell adhesion is weak. In contrast, cells on the ABM/P-15 surface (with or without hydrogel) had more actin filaments and stress fibers, suggesting that P-15 coating on ABM promotes and strengthens cell adhesion.

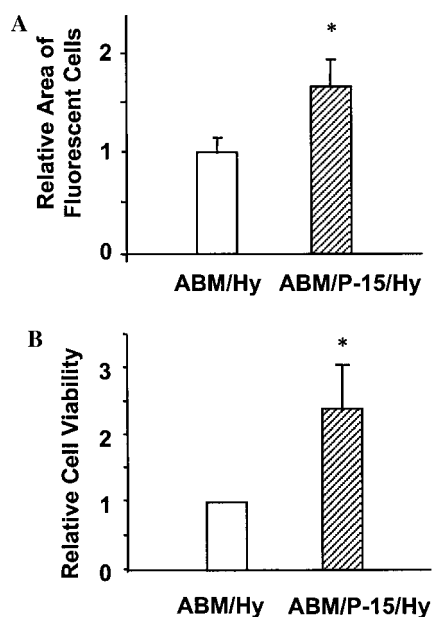


Fig. 3. Quantitative measurement of cell attachment and viability on ABM/Hy and ABM/P-15/Hy. (A) HOS cells were labeled with DiI for 5 min and plated on ABM/Hy and ABM/P-15/Hy for 24 h. The images of fluorescent cells on the particles were collected by fluorescence microscopy as shown in Fig. 2. The area covered by fluorescent cells in the images was quantified by NIH Image software. Data are presented as means \pm SE from three experiments. *Significant difference ($p < 0.05$) in the relative area covered by fluorescent cells when compared with ABM/Hy. (B) Cell viability on ABM/Hy and ABM/P-15/Hy. HOS cells were plated on the ABM/Hy and ABM/P-15/Hy. After 4 days, MTT was added to the culture medium for 4 h. The cells were lysed and used for MTT assay. The ABM/Hy samples were used as the reference for the normalization in each experiment. Data are presented as means \pm SE from three experiments. *Significant difference ($p < 0.05$) when compared with ABM/Hy samples.

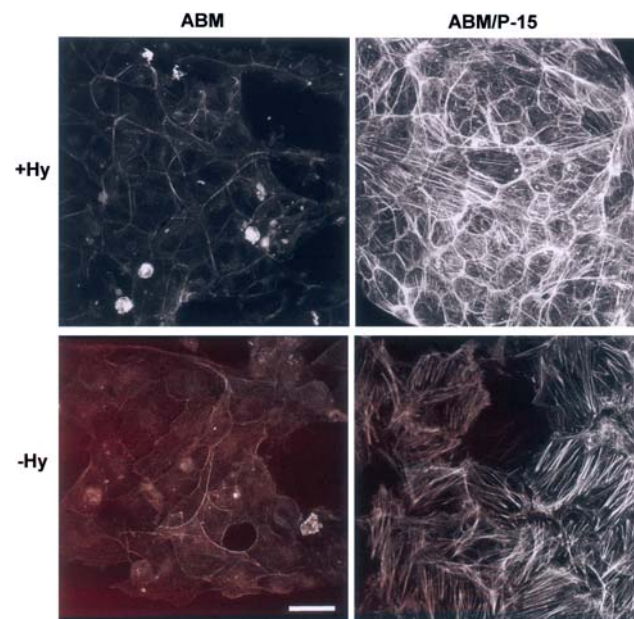


Fig. 4. Effect of P-15 on actin cytoskeleton in cells on the ABM surface. HOS cells were plated on ABM/Hy, ABM/P-15/Hy, ABM, and ABM/P-15 particles immobilized on poly-HEMA-coated surface. After 24 h, the cells were fixed and stained on actin filaments with FITC-phalloidin for 1 h. The images of cells on the particles were collected by confocal microscopy and the optical sections for each field were projected onto a plane. Representative images from three experiments are shown here. Same hardware and software settings were used to collect the images for different samples. Bar = 50 μ m.

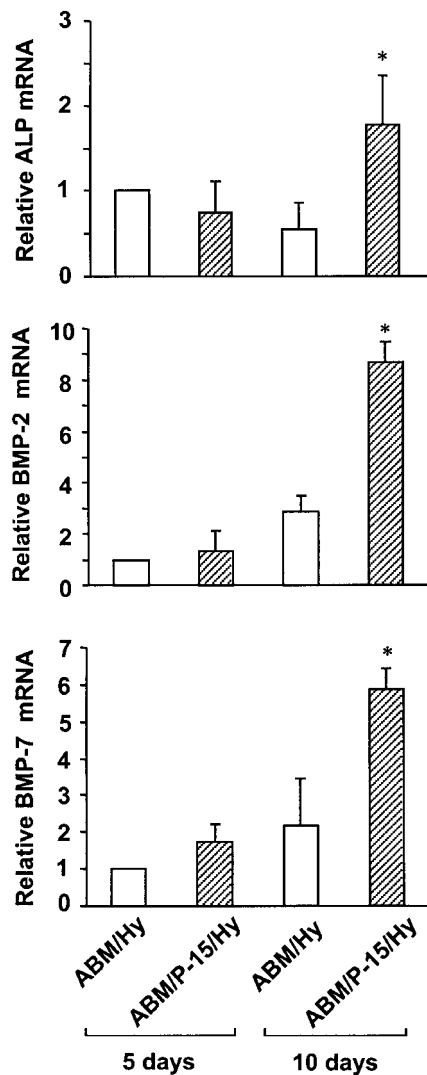


Fig. 5. Osteoblastic gene expression in HOS cells on ABM/Hy and ABM/P-15/Hy. HOS cells were seeded on the ABM/Hy and ABM/P-15/Hy. The cells were cultured for 5 or 10 days and lysed for RNA isolation. The RNA from each sample was reverse-transcribed into cDNA and the expression of each gene was analyzed by real time qPCR with respective primers. The expression level of each gene was normalized with the level of GAPDH in the same sample. Data are presented as means \pm SE from three experiments. *Significant difference ($p < 0.05$) when compared with ABM/Hy samples.

Increased osteoblastic gene expression with ABM/P-15/Hy

The effects of P-15 on osteoblastic activity in HOS cells cultured on ABM/Hy or ABM/P-15/Hy for 5 or 10 days were determined by gene expression analysis. The RNA was isolated and the expression levels of three genes involved in osteoblastic differentiation were analyzed: ALP, BMP-2, and BMP-7 (Fig. 5). After 5-day culture, there was no significant difference of these osteoblastic genes in cells grown on ABM/Hy and ABM/P-15/Hy. However, after 10 days, the gene expression of ALP, BMP-2 and BMP-7 in cells grown on ABM/P-15/Hy was significantly higher than that of cells on ABM/Hy. The up-regulation of these genes suggests that P-15 promotes the osteoblastic activity in HOS cells.

Increased deposition of mineralized matrix with ABM/P-15/Hy

HOS cells were cultured on ABM/Hy and ABM/P-15/Hy for 2 weeks and then stained with Alizarin Red. As shown in Fig. 6, the deposition of mineral matrix (in red) on ABM/P-15/Hy particles was more than that on ABM/Hy. These results suggest that ABM/P-15 in Hy can increase the deposition of mineral matrix, which is consistent with the effects of ABM/P-15/Hy on osteoblastic gene expression (Fig. 5).

Cell attachment on CMC and alginate hydrogel-suspended ABM/P-15 particles

We also determined whether other hydrogels affect the biomimetic activity of ABM/P-15. ABM and ABM/P-15 particles were suspended in alginate or CMC hydrogels and spread onto culture surface, followed by cell seeding. After 24 h, HOS cells attached on ABM/P-15/hydrogels were approximately twice the amount of cells attached on ABM particles in both hydrogels (Fig. 7). The increase of cell attachment in the presence of P-15 is consistent with the approximate twofold increase obtained with the Hy hydrogel (Fig. 3). These results suggest that

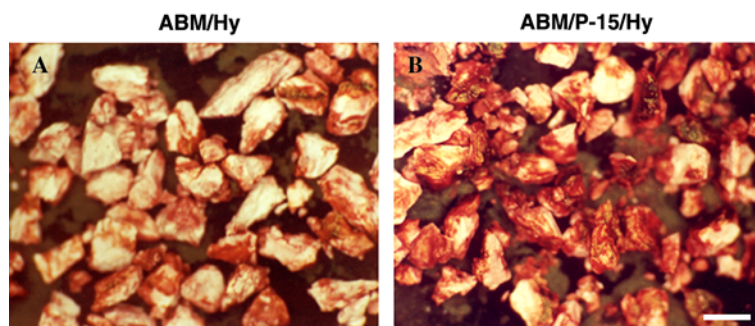


Fig. 6. Alizarin Red staining of mineralized matrix in ABM/Hy and ABM/P-15/Hy. HOS cells were plated on Hy hydrogels embedded with ABM (A) or ABM/P-15 (B) particles and allowed to grow for 2 weeks. After washing away unbound cells and hydrogels, the specimens were fixed and stained with 2% Alizarin Red S. Bar = 500 μ m. (For interpretation of the reference to colour, the reader is referred to the web version of this paper.)

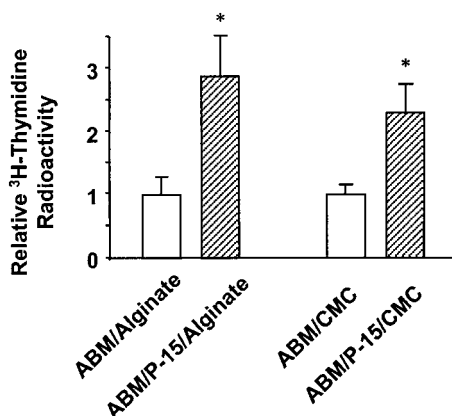


Fig. 7. Effect of P-15 on cell attachment on ABM particles in CMC and alginate hydrogels. HOS cells were radiolabeled with [³H]thymidine for 36 h and plated on CMC or alginate hydrogels embedded with ABM or ABM/P-15 particles. After 24 h, unbound cells and hydrogels were washed away and cells on ABM or ABM/P-15 particles were lysed. The [³H]thymidine radioactivity (an index of cell numbers) was measured by using a scintillation counter. Data are presented as means \pm SE from three experiments. *Significant difference ($p < 0.05$) when compared with ABM/hydrogel samples.

P-15 enhances cell adhesion on the ABM matrix in the presence of hydrogels—Hy, CMC or alginate.

Increased deposition of mineralized matrix with ABM/P-15/CMC

To test whether HOS had enhanced mineralized matrix deposition on ABM/P-15/CMC as that on ABM/P-15/Hy (Fig. 6), HOS cells were cultured on ABM/CMC and ABM/P-15/CMC for 2 weeks, and then stained with Alizarin Red. As shown in Fig. 8, the deposition of mineral matrix (in red) on ABM/P-15/CMC particles was more than that on ABM/CMC.

Discussion

During the repair and remodeling in skeletal structures, the early deposition of collagenous matrix is part

of the repair process in tissues. Reparative cells migrate on this matrix, and subsequently organize and remodel the matrix through cytoskeleton and matrix synthesis/degradation. P-15-coated ABM surfaces simulate the role of native collagen matrix in wound repair. ABM/P-15 in different types of hydrogels (Hy, CMC, and alginate) has more HOS cell attachment in comparison to the hydrogel-suspended ABM without P-15 (Figs. 2, 3, and 7). P-15 increases actin stress fibers in cells attached on the ABM surface (Fig. 4), suggesting enhanced cell adhesion and matrix remodeling. Cells cultured on ABM/P-15/Hy have increased osteogenic gene expression for alkaline phosphatase, BMP-2 and BMP-7, and ABM/P-15 in hydrogels promote matrix mineralization. These results showed that hydrogels containing ABM/P-15 enhanced cell adhesion and osteoblastic activity, and can be used as an injectable biomimetic matrix to facilitate the repair of bone defects.

The presence of P-15 peptide increases the gene expression of BMP-2 and BMP-7—the osteogenic factors that have been reported to stimulate osteoblastic activity [27–29] through autocrine or paracrine mechanisms. In addition to the direct effect of P-15 on BMP expression, P-15 peptide may synergize the effects of osteogenic factors to induce osteoblastic differentiation. There is evidence that BMPs and TGF- β collaborate with collagen to induce osteoblastic activity [11,30–32]. Alternatively, P-15 peptide may modulate signaling pathways and make the cells more sensitive to osteogenic factors. For example, collagen integrin receptors mediate osteoblast differentiation induced by BMP-2 [31], and collagen can alter the activity of protein kinase C and increase cAMP level in response to parathyroid hormone [9].

The synthesized P-15 peptide has advantage over the use of reconstituted collagen in many aspects. First, P-15 peptide can be synthesized in large scale with low expenses and little variation between different batches; this approach avoids the tedious procedure in the purification of collagen, which may exhibit inconsistency in

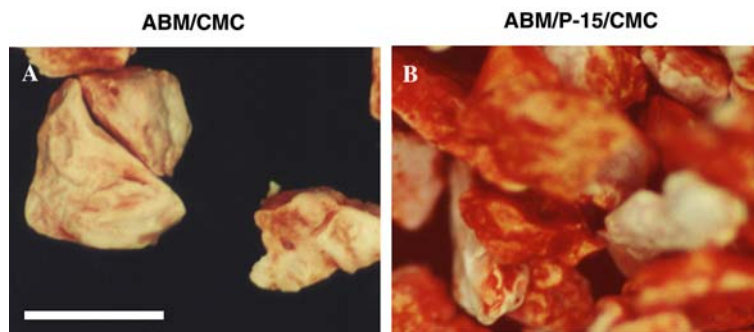


Fig. 8. Alizarin Red staining of mineralized matrix in ABM/CMC and ABM/P-15/CMC. HOS cells were cultured for 2 weeks on CMC hydrogels embedded with ABM (A) or ABM/P-15 (B) particles. After washing away unbound cells and hydrogels, the specimens were fixed and stained with 2% Alizarin Red S. Bar = 500 μ m. (For interpretation of the reference to colour, the reader is referred to the web version of this paper.)

collagen quality and have risks of transferring pathogen from the tissue donors. Second, P-15 peptide is more stable than collagen molecule and is easier to handle. P-15 has a long shelf life, both as free and immobilized peptide, and does not require special handling and storage procedures. P-15 and its biomaterial composites can be sterilized easily by autoclaving, by UV, or by γ -irradiation. Finally, P-15 peptide mimics the bioactivity of collagen in cell adhesion and differentiation, but does not induce inflammatory responses as reconstituted collagen [33–35]. Additionally, P-15 peptide bound to biomaterials promotes the attachment of reparative cells from the host and enhances the coverage of material surfaces by the cells and the newly deposited ECM, which may help to mask the “foreign” materials and decrease foreign body responses.

The results of this study suggest that hydrogel composition (Hy, CMC, and alginate) does not alter the effects of P-15 peptide on cell attachment and osteoblastic differentiation on ABM mineral matrix. The suspension of ABM/P-15 in hydrogel will make it easier to deliver and maintain the graft in osseous defects or gaps during surgery.

Acknowledgments

We thank Dr. Andrew J. Tofe, Julia Chu, Dana F. Lee, and Diana X. Yu for their excellent technical support. This study was supported by a research grant from Whitaker Foundation and funding from CeraPedics, L.L.C and Tescient, Inc.

References

- [1] J.W. Karesh, Biomaterials in ophthalmic plastic and reconstructive surgery, *Curr. Opin. Ophthalmol.* 9 (1998) 66–74.
- [2] J.A. Hubbell, Bioactive biomaterials, *Curr. Opin. Biotechnol.* 10 (1999) 123–129.
- [3] E. Ruoslahti, M.D. Pierschbacher, New perspectives in cell adhesion: RGD and integrins, *Science* 238 (1987) 491–497.
- [4] Y. Ito, M. Kajihara, Y. Imanishi, Materials for enhancing cell adhesion by immobilization of cell-adhesive peptide, *J. Biomed. Mater. Res.* 25 (1991) 1325–1337.
- [5] H.K. Kleinman, R.J. Klebe, G.R. Martin, Role of collagenous matrices in the adhesion and growth of cells, *J. Cell Biol.* 88 (1981) 473–485.
- [6] S.C. Strom, G. Michalopoulos, Collagen as a substrate for cell growth and differentiation, *Methods Enzymol.* 82 (Part A) (1982) 544–555.
- [7] G. Maor, K. von der Mark, H. Reddi, D. Heinegard, A. Franzen, M. Silbermann, Acceleration of cartilage and bone differentiation on collagenous substrata, *Coll. Relat. Res.* 7 (1987) 351–370.
- [8] C.M. Serre, M. Papillard, P. Chavassieux, G. Boivin, In vitro induction of a calcifying matrix by biomaterials constituted of collagen and/or hydroxyapatite: an ultrastructural comparison of three types of biomaterials, *Biomaterials* 14 (1993) 97–106.
- [9] J. Green, S. Schotland, D.J. Stauber, C.R. Kleeman, T.L. Clemens, Cell–matrix interaction in bone: type I collagen modulates signal transduction in osteoblast-like cells, *Am. J. Physiol.* 268 (1995) C1090–C1103.
- [10] Y. Takeuchi, K. Nakayama, T. Matsumoto, Differentiation and cell surface expression of transforming growth factor- β receptors are regulated by interaction with matrix collagen in murine osteoblastic cells, *J. Biol. Chem.* 271 (1996) 3938–3944.
- [11] M. Mizuno, Y. Kuboki, TGF- β accelerated the osteogenic differentiation of bone marrow cells induced by collagen matrix, *Biochem. Biophys. Res. Commun.* 211 (1995) 1091–1098.
- [12] R.S. Bhatnagar, J.J. Qian, C.A. Gough, The role in cell binding of a β -bend within the triple helical region in collagen $\alpha 1$ (I) chain: structural and biological evidence for conformational tautomerism on fiber surface, *J. Biomol. Struct. Dyn.* 14 (1997) 547–560.
- [13] R.S. Bhatnagar, J.J. Qian, A. Wedrychowska, M. Sadeghi, Y.M. Wu, N. Smith, Design of biomimetic habitats for tissue engineering with P-15, a synthetic peptide analogue of collagen, *Tissue Eng.* 5 (1999) 53–65.
- [14] R.A. Yukna, D.P. Callan, J.T. Krauser, G.H. Evans, M.E. Aichelmann-Reidy, K. Moore, R. Cruz, J.B. Scott, Multi-center clinical evaluation of combination anorganic bovine-derived hydroxyapatite matrix (ABM)/cell binding peptide (P-15) as a bone replacement graft material in human periodontal osseous defects: 6-month results, *J. Periodontol.* 69 (1998) 655–663.
- [15] R.A. Yukna, J.T. Krauser, D.P. Callan, G.H. Evans, R. Cruz, M. Martin, Multi-center clinical comparison of combination anorganic bovine-derived hydroxyapatite matrix (ABM)/cell binding peptide (P-15) and ABM in human periodontal osseous defects: 6-month results, *J. Periodontol.* 71 (2000) 1671–1679.
- [16] F.S. Panagakos, C. Fernandez, S. Kumar, Ultrastructural analysis of mineralized matrix from human osteoblastic cells: effect of tumor necrosis factor- α , *Mol. Cell. Biochem.* 158 (1996) 81–89.
- [17] K. Okamoto, T. Matsuura, R. Hosokawa, Y. Akagawa, RGD peptides regulate the specific adhesion scheme of osteoblasts to hydroxyapatite but not to titanium, *J. Dent. Res.* 77 (1998) 481–487.
- [18] M.E. Gomes, R.L. Reis, A.M. Cunha, C.A. Blitterswijk, J.D. de Bruijn, Cytocompatibility and response of osteoblastic-like cells to starch-based polymers: effect of several additives and processing conditions, *Biomaterials* 22 (2001) 1911–1917.
- [19] B.A. Scheven, D. Marshall, R.M. Aspdin, In vitro behaviour of human osteoblasts on dentin and bone, *Cell Biol. Int.* 26 (2002) 337–346.
- [20] A.M. Sun, G.M. O’Shea, M.F. Goosen, Injectable microencapsulated islet cells as a bioartificial pancreas, *Appl. Biochem. Biotechnol.* 10 (1984) 87–99.
- [21] A.S. Sawhney, C.P. Pathak, J.A. Hubbell, Interfacial photopolymerization of poly(ethylene glycol)-based hydrogels upon alginate-poly(L-lysine) microcapsules for enhanced biocompatibility, *Biomaterials* 14 (1993) 1008–1016.
- [22] J.A. Rowley, G. Madlambayan, D.J. Mooney, Alginate hydrogels as synthetic extracellular matrix materials, *Biomaterials* 20 (1999) 45–53.
- [23] J.L. West, S.M. Chowdhury, A.S. Sawhney, C.P. Pathak, R.C. Dunn, J.A. Hubbell, Efficacy of adhesion barriers. Resorbable hydrogel, oxidized regenerated cellulose and hyaluronic acid, *J. Reprod. Med.* 41 (1996) 149–154.
- [24] J. Trudel, S.P. Massia, Assessment of the cytotoxicity of photo-crosslinked dextran and hyaluronan-based hydrogels to vascular smooth muscle cells, *Biomaterials* 23 (2002) 3299–3307.
- [25] S. Schneider, P.J. Feilen, V. Slotty, D. Kampfner, S. Preuss, S. Berger, J. Beyer, R. Pommersheim, Multilayer capsules: a promising microencapsulation system for transplantation of pancreatic islets, *Biomaterials* 22 (2001) 1961–1970.
- [26] J.J. Qian, R.S. Bhatnagar, Enhanced cell attachment to anorganic bone mineral in the presence of a synthetic peptide related to collagen, *J. Biomed. Mater. Res.* 31 (1996) 545–554.
- [27] M.R. Urist, R.J. DeLange, G.A. Finerman, Bone cell differentiation and growth factors, *Science* 220 (1983) 680–686.

- [28] A.H. Reddi, Role of morphogenetic proteins in skeletal tissue engineering and regeneration, *Nat. Biotechnol.* 16 (1998) 247–252.
- [29] U. Ripamonti, A.H. Reddi, Growth and morphogenetic factors in bone induction: role of osteogenin and related bone morphogenetic proteins in craniofacial and periodontal bone repair, *Crit. Rev. Oral Biol. Med.* 3 (1992) 1–14.
- [30] K. Takaoka, H. Nakahara, H. Yoshikawa, K. Masuhara, T. Tsuda, K. Ono, Ectopic bone induction on and in porous hydroxyapatite combined with collagen and bone morphogenetic protein, *Clin. Orthop.* (1988) 250–254.
- [31] A. Jikko, S.E. Harris, D. Chen, D.L. Mendrick, C.H. Damsky, Collagen integrin receptors regulate early osteoblast differentiation induced by BMP-2, *J. Bone Miner. Res.* 14 (1999) 1075–1083.
- [32] N. Muthukumaran, S. Ma, A.H. Reddi, Dose-dependence of and threshold for optimal bone induction by collagenous bone matrix and osteogenin-enriched fraction, *Coll. Relat. Res.* 8 (1988) 433–441.
- [33] F. DeLustro, R.A. Condell, M.A. Nguyen, J.M. McPherson, A comparative study of the biologic and immunologic response to medical devices derived from dermal collagen, *J. Biomed. Mater. Res.* 20 (1986) 109–120.
- [34] L.R. Ellingsworth, F. DeLustro, J.E. Brennan, S. Sawamura, J. McPherson, The human immune response to reconstituted bovine collagen, *J. Immunol.* 136 (1986) 877–882.
- [35] K.R. Meade, F.H. Silver, Immunogenicity of collagenous implants, *Biomaterials* 11 (1990) 176–180.